TYPE 1 DIABETES

Partial exhaustion of CD8 T cells and clinical response to teplizumab in new-onset type 1 diabetes

S. Alice Long,[1] Jerill Thorpe,[1] Hannah A. DeBerg,[2] Vivian Gersuk,[2] James A. Eddy,[2] Kristina M. Harris,[3] Mario Ehlers,[4] Kevan C. Herold,[5] Gerald T. Nepom,[3] Peter S. Linsley[2]*

Biologic treatment of type 1 diabetes (T1D) typically results in transient stabilization of C-peptide levels (a surrogate for endogenous insulin secretion) in some patients, followed by progression at the same rate as in untreated control groups. We used integrated systems biology and flow cytometry approaches with clinical trial blood samples to elucidate pathways associated with C-peptide stabilization in T1D patients treated with the anti-CD3 monoclonal antibody teplizumab. We identified a population of CD8 T cells that accumulated in patients with the best response to treatment (responders) and showed that these cells phenotypically resembled exhausted T cells by expressing high levels of the transcription factor EOMES, effector molecules, and multiple inhibitory receptors (IRs), including TIGIT and KLRG1. These cells expanded after treatment, with levels peaking after 3 to 6 months. To functionally characterize these exhausted-like T cells, we isolated memory CD8 TIGIT$^+$KLRG1$^+$ T cells from responders and showed that they exhibited expanded T cell receptor clonotypes (indicative of previous in vivo expansion), recognized a broad-based spectrum of environmental antigens and autoantigens, and were hypoproliferative during polyclonal stimulation, increasing expression of IR genes and decreasing cell cycle genes. Triggering these cells with a recombinant ligand for TIGIT during polyclonal stimulation further down-regulated their activation, demonstrating that their exhausted phenotype was not terminal. These findings identify and functionally characterize a partially exhausted cell type associated with response to teplizumab therapy and suggest that pathways regulating T cell exhaustion may play a role in successful immune interventions for T1D.

INTRODUCTION

The therapeutic goal for type 1 diabetes (T1D) is to preserve β cell function, commonly monitored by measuring C-peptide levels. Biologic therapies with distinct immunologic mechanisms of action, including anti-CD3 (otelixizumab and teplizumab), anti-CD20 (rituximab), and costimulation blockade (abatacept), are partially effective in individuals newly diagnosed with T1D (*1*, *2*). Because T cells play a key role in the pathophysiology of T1D (*3*), much of the effort in finding new therapies has been directed toward inducing T cell unresponsiveness (tolerance) (*1*). Multiple mechanisms have been associated with T cell tolerance in research settings (*4*, *5*), but this knowledge has not yet led to long-term therapeutic benefit in T1D (*1*). One mechanism that can lead to T cell unresponsiveness in vivo is T cell exhaustion (*4*, *6*, *9*–*11*). Exhausted T cells are characterized by loss of effector functions (cytokine production and proliferation), expression of multiple inhibitory receptors (IRs), differential connectivity of transcription factors, low metabolic activity, and dependence on continuous presence of antigen (*4*, *6*, *9*–*11*). Recently, T cell exhaustion was identified as a beneficial prognostic indicator in several autoimmune diseases (*12*).

Transcriptomic measurements are widely used for unbiased mechanistic studies and for biomarker identification. These studies have been particularly successful with cancer, where large data sets comprising hundreds to thousands of samples are freely available to the research community (*7*). These big data approaches have been more challenging in T1D studies, in part because of difficulties in accessing the primary diseased tissue. Instead, because blood collection is more practical, numerous investigators have focused on classification of T1D patients using transcriptome profiling of whole-blood and leukocyte populations. Although whole-blood signatures have been identified in patients with T1D relative to controls (*13*), little is known about transcript signatures associated with response to therapy.

To identify mechanisms involved in the preservation of β cell function, we used a systems biology approach to interrogate samples from the AbATE (Autoimmunity-Blocking Antibody for Tolerance) study, a randomized controlled clinical trial of teplizumab treatment in new-onset T1D (*14*). This was a longitudinal study with samples collected from the same individual at multiple time points. Furthermore, individuals were synchronized in time relative to the onset of T1D, and clinical phenotypes, such as C-peptide levels, were measured at each collection time point. Here, we used unbiased whole-blood transcriptomic approaches to identify cellular and molecular markers that accompanied successful treatment with a non–Fc-binding anti-CD3 monoclonal antibody (mAb; teplizumab) (*14*). We describe an EOMES-associated transcriptional signature that is associated with maintenance of C-peptide and is expressed by memory CD8 T cells that phenotypically and functionally resemble partially exhausted T cells, suggesting their role in tolerance induction.

RESULTS

Expression of EOMES-associated genes is correlated with C-peptide levels

AbATE was a randomized controlled trial designed (fig. S1) to determine whether two 14-day courses of treatment with teplizumab a year apart would reduce the decline in C-peptide levels in T1D patients 2 years after disease onset (*14*). The study included 25 untreated control patients, all of whom showed ≥40% loss of baseline C-peptide levels, measured as mean area under the curve (AUC) in a 4-hour mixed-meal tolerance test. The teplizumab-treated group

[1]Translational Research Program, Benaroya Research Institute, Seattle, WA 98101, USA. [2]Systems Immunology, Benaroya Research Institute, Seattle, WA 98101, USA. [3]Immune Tolerance Network, Bethesda, MD 20814, USA. [4]Immune Tolerance Network, San Francisco, CA 94107, USA. [5]Departments of Immunobiology and Internal Medicine, Yale University, New Haven, CT 06520, USA.
*Corresponding author. Email: plinsley@benaroyaresearch.org

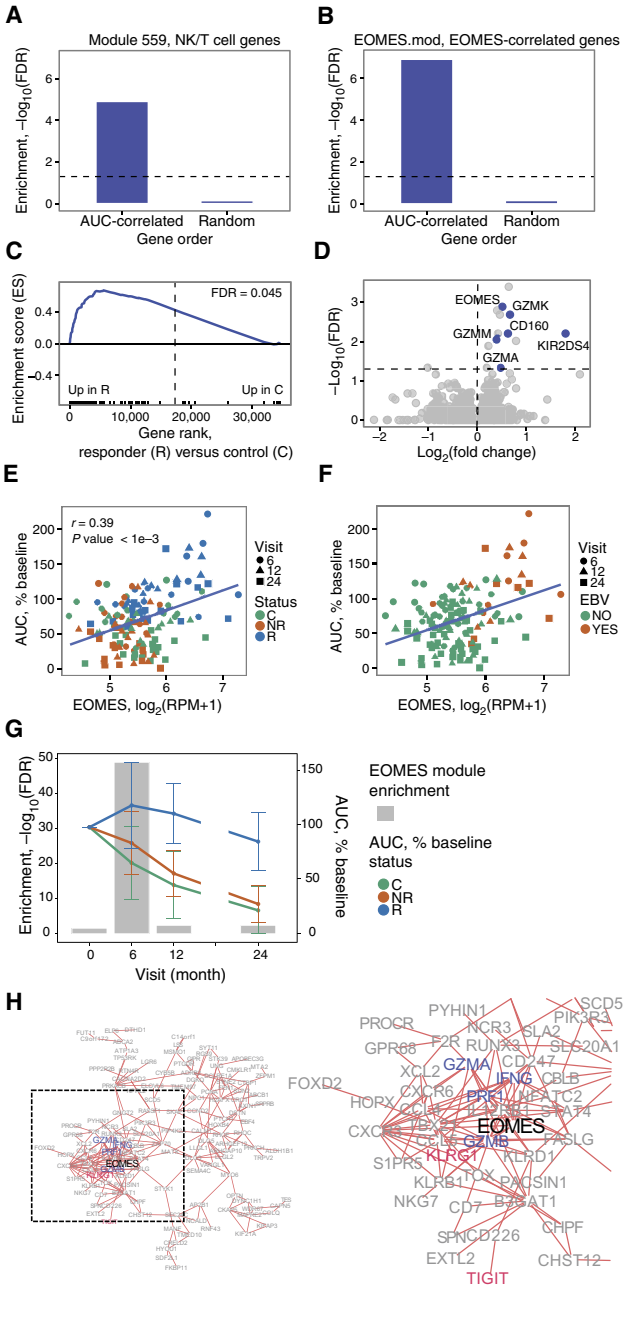

Fig. 1. An NK/T cell, *EOMES*-associated gene signature was detected in whole blood of teplizumab R patients. (**A** and **B**) Bar plots of the overlap between module 559 (A) or EOMES.mod (B) and the 400 top C-peptide–correlated or randomly ordered genes. Dashed line, FDR = 0.05. (**C**) Blue line, enrichment score for overrepresentation of EOMES.mod genes in a list of all genes ranked by expression in R samples versus C samples; solid vertical black lines, positions of EOMES.mod genes in the ranked list; dashed vertical line, median number of genes. (**D**) Differential gene expression for R patients versus C patients. Blue dots, selected NK/CD8 T cell genes; gray dots, all other genes. Horizontal dashed line, FDR = 0.05; vertical dashed line, $\log_2$(fold change) = 0. (**E**) EOMES gene expression versus AUC. The *P* value was calculated using independent permutation analysis of samples from each visit. (**F**) EOMES expression versus AUC, colored by EBV reactivation. RPM, reads per million. (**G**) Overlap of AUC-correlated genes (n = 300; table S2) with the top 300 EOMES-associated genes. The right *y* axis shows C-peptide AUC levels (means ± SD). (**H**) Left: A protein-protein interaction network of the 300 genes most highly correlated with EOMES expression. Right: Expanded view of the boxed area.

(n = 49 of the 52 total patients who could be evaluated) comprised 27 patients (55%), whose C-peptide also declined by ≥40% (termed nonresponders), and 22 patients (44%), who lost <40% of baseline AUC (termed responders). Here, we use the abbreviations R, NR, and C to refer to responders, nonresponders, and untreated controls, respectively. The numbers and characteristics of samples used for each of the approaches utilized are described in table S1.

We first tested the feasibility of systems approaches to this problem by conducting microarray analysis on whole-blood samples of patients from the 12-month visit when C-peptide differences between the groups were the greatest but before treatment with the second course of teplizumab. To search for differences at the level of biological processes associated with networks of genes, we monitored levels of immune cells and pathways using predefined sets (modules) of co-regulated immune genes (*15*) using modular approaches. Because C-peptide AUC is commonly used as a marker of T1D progression (*2*), we reasoned that genes and pathways whose expression was most correlated with AUC would include genes involved in β cell preservation. Our experimental approach to test this hypothesis is outlined in fig. S2.

We ranked all genes by correlation with AUC and then tested for pathways overrepresented in the most highly correlated genes testing for gene overlap with predefined gene modules (*15*, *16*). We first tested AUC-correlated genes for overlap with a set of modules defined by expression in different hematopoietic cell types (*16*). This analysis revealed a single module of natural killer (NK)/T cell genes [previously termed "module 559" (*16*)] that overlapped significantly with a range of set sizes for AUC-correlated genes (fig. S3). A plot from one representative set size is shown in Fig. 1A. Overlapping genes included cytotoxic genes (*GZMA*, *GZMH*, and *GZMK*) and cell surface markers common to both CD8 T cells and NK cells (*CD160* and *NKG7*). When an equivalent set size of genes arranged in random order was used (Fig. 1A), none of the modules showed significant overlap. Thus, CD8 T cell and NK cell genes were most strongly associated with C-peptide levels.

To further characterize pathways, processes, and cell types correlated with C-peptide levels, we extended the analysis of AUC-correlated genes to a second set of immune modules, termed immune marker modules (*15*). This set of modules comprised the top genes correlated with various hematopoietic cell CD molecules, cytokines, and transcription factors in an immune cell gene expression atlas (*15*). Genes in each module were not necessarily unique, and many of the modules shared genes (*15*). When tested against AUC-correlated genes, numerous modules showed significant overlap (fig. S3). The most significant overlap was seen with a module of genes associated with the transcription factor *EOMES* (EOMES.mod; Fig. 1B) and with other gene modules (n = 12) that shared significant numbers of genes (fig. S3) with EOMES.mod (all showed >~5% overlap, hypergeometric $P \leq 1.5 \times 10^{-7}$). Modules not significantly overlapping with EOMES.mod (n = 98) did not show significant overlap with AUC-correlated genes (fig. S3). Moreover, none of the modules showed coherent and significant overlap with randomly ranked genes (fig. S3 and Fig. 1B). Together, these findings indicate that several modules sharing significant numbers of genes with EOMES.mod were enriched in AUC-correlated genes. Because *EOMES* and *EOMES*-associated genes consistently scored near the top in many different analyses in our

studies (Fig. 1), we selected *EOMES*-correlated genes (table S2) as a prototype gene set to use in subsequent studies, focusing on the top 100 to 300 *EOMES*-associated genes.

EOMES-associated gene levels correlate with the R phenotype

After identifying an *EOMES*-associated signature across all samples, we tested for association of the signature with the different patient groups using gene set enrichment analysis (GSEA) (*17*). We quantified enrichment of immune molecular modules (*15*) in gene lists ranked by expression in R versus C or R versus NR. EOMES.mod and other modules sharing significant numbers of genes were found to have high enrichment scores coupled with high $-\log_{10}$ false discovery rate (FDR) or lowest corrected $-P$ values, indicating preferential association with R samples versus C samples (fig. S4). EOMES.mod genes were significantly associated with R, as compared with C (Fig. 1C). These findings indicate that elevated levels of *EOMES*-associated genes were associated with the R phenotype.

EOMES-associated gene expression correlates with C-peptide kinetics

To determine temporal changes in *EOMES*-associated gene expression, we expanded our analysis to include all available whole-blood RNA samples in the AbATE study (0-, 6-, 12-, and 24-month visits; table S1). For these expanded studies, we used RNA sequencing (RNA-seq) technology, which is rapidly supplanting microarray analysis as the method of choice for transcriptomic analysis (*18*). Consistent with the microarray analysis, we detected increased expression of *EOMES* and several other CD8 T cell/NK cell genes in R samples (Fig. 1D). By comparing *EOMES* transcript to clinical outcomes, we found that levels of *EOMES* transcript were significantly correlated with AUC across all samples (Fig. 1E), most strongly in R samples. We also found that levels of *EOMES* transcript and AUC were significantly correlated with Epstein-Barr virus (EBV) reactivation, indicating that failure to control EBV is associated with increased expression of *EOMES* (Fig. 1F).

The kinetics of the *EOMES*-associated gene up-regulation was examined by detecting their enrichment in AUC-correlated genes at each individual timed visit (Fig. 1G). Enrichment of *EOMES*-associated genes after the first course of treatment was greatest at the 6-month visit and decreased at the 12- and 24-month visits. Because RNA samples from the 18-month visit were not available, we could not determine how gene expression levels were affected by the second course of therapy. Changes in expression of *EOMES*-associated genes paralleled the changes in C-peptide levels observed clinically (Fig. 1G).

To test interconnectedness of *EOMES*-associated genes, we projected them onto a protein-protein interaction network (*19*). The resulting network graph (Fig. 1H) showed that *EOMES*-associated genes comprised a highly interconnected set of proteins and were highly enriched in genes having known interactions (FDR $< 2 \times 10^{-16}$). The network was also significantly enriched for genes annotated with the KEGG (Kyoto Encyclopedia of Genes and Genomes) term "Natural killer cell mediated cytotoxicity" (FDR $= 2.9 \times 10^{-4}$) and contained both effector molecules (*GZMA*, *GZMB*, *PRF1*, and *IFNG*) and IRs (*KLRG1* and *TIGIT*).

R patients display increased levels of CD8 T cells expressing *EOMES*-associated genes

To determine what cell types were best correlated with *EOMES* mRNA, we performed a comparison of *EOMES* expression levels by RNA-seq with frequencies of various cell types determined by flow cytometry tests conducted on peripheral blood mononuclear cell (PBMC) samples from the same visits (*20*). Of all the populations tested ($n = 33$), *EOMES* levels were best correlated with levels of CD8 memory T cells ($r = 0.71$) and more weakly with NK cells ($r = 0.33$) (fig. S5).

To better determine what cell types express *EOMES*-associated genes, we augmented our gene expression analysis with in-depth flow cytometry analysis. We interrogated cryopreserved PBMCs by flow cytometry using panels of mAbs targeting cell subset markers and selected proteins encoded by *EOMES*-associated genes (table S3). We began by performing a broad univariate analysis, followed by coexpression analyses, and then focused longitudinal analyses (fig. S6).

We first compared patients who exhibited extreme *EOMES*-high (mostly R patients) and *EOMES*-low (mostly NR patients) gene expression profiles (table S1). We used both mean fluorescence intensity (MFI) and percent positive cells as metrics for single-cell marker expression. As shown in Fig. 2A, MFI for the IRs TIGIT, KLRG1, and CD160 was increased on CD8 T cells, yet EOMES protein levels did not differ significantly with any cell type. In contrast, both the overall fold change and significance of expression differences were greater when percentages of positive cells were measured (compare Fig. 2, A and B). The proportion of memory CD8 and, to a lesser extent, naive CD8 T cells expressing EOMES and other signature proteins increased most significantly in *EOMES*-high patients (Fig. 2B). An example of the increase in percentage of cells coexpressing *EOMES*-associated proteins in selected *EOMES*-high versus *EOMES*-low patients is shown in Fig. 2C.

Because of the high level of expression of TIGIT and KLRG1 proteins and their strong association with EOMES protein, we measured the coexpression of TIGIT and KLRG1 proteins on total CD8 T cells in peripheral blood over time (Fig. 2D). When analyzed across the entire AbATE study, percentages of $TIGIT^+KLRG1^+$ CD8 T cells increased after both treatment courses (Fig. 2D), reaching a maximum of 3 to 6 months in R patients after each course of treatment. Percentages of $TIGIT^+KLRG1^+$ CD8 T cells increased to a lesser extent in NR patients and remained constant in C patients. Last, we analyzed the composition of $TIGIT^+KLRG1^+$ CD8 T cells in R patients over time and found no evidence of selective expansion of a specific subtype of differentiation (Fig. 2E). Together, these findings demonstrate that percentages of CD8 T cells expressing certain EOMES-associated proteins in peripheral blood increased in R patients after teplizumab treatment.

CD8 T cells expressing *EOMES* network genes display a restricted TCR usage

Although CD8 memory cells expressed EOMES, TIGIT, and KLRG1 proteins by flow cytometry, the extent to which they expressed the full set of *EOMES*-associated genes was not known. To better characterize expression of *EOMES* network genes, we isolated $CD45RO^+TIGIT^+KLRG1^+$ CD8 T cells [double high (DH)] from R patients after the first course of treatment at month 6 ($n = 3$) (Fig. 3A). For comparison, we isolated $CD45RO^+TIGIT^-KLRG1^-$ CD8 T cells [double low (DL)] from the same patients. We then performed low-input bulk RNA-seq on replicate samples from both populations and compared expression of the full *EOMES*-associated gene set. DH cells expressed higher levels of *EOMES* network genes (Fig. 3B). Nearly all the *EOMES*-associated genes (~95%) were expressed in DH cells,

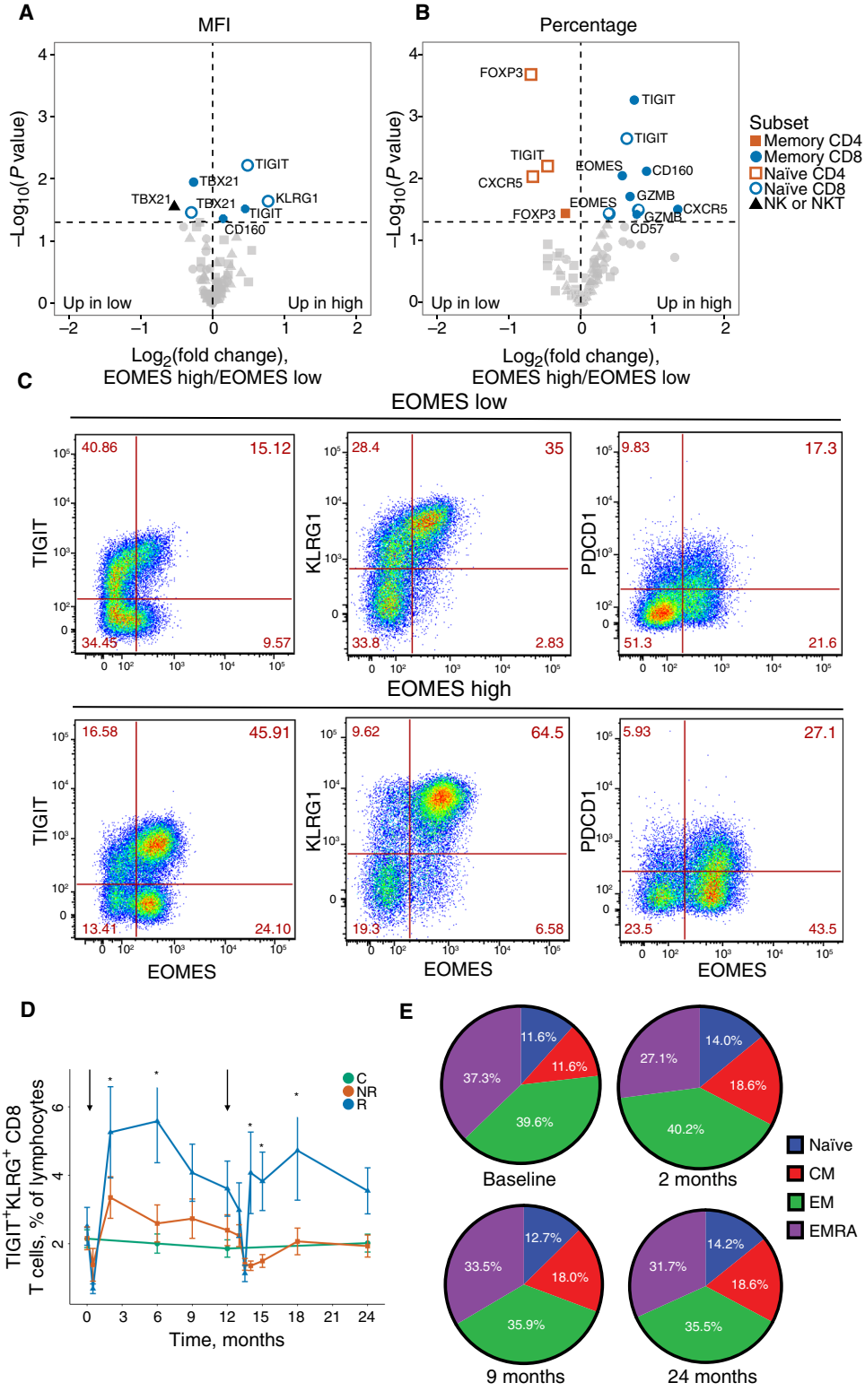

Fig. 2. Accumulation of a CD8 cell subset in R patients marked by EOMES, KLRG1, and TIGIT protein expression. (**A** and **B**) Differential surface expression of MFI (A) and percentages of marker-positive cells (B) in the parent lymphocyte populations. *Y* axis, $-\log_{10}$ (uncorrected *P* value) of difference between *EOMES*-high groups versus *EOMES*-low groups; *x* axis, $\log_2$ fold change of differences. Dashed horizontal line, $P = 0.05$; dashed vertical line, log(fold change) = 0. (**C**) Coexpression of EOMES with TIGIT, KLRG1, or PDCD1 in memory CD8 T cells from EOMES-high (bottom) and EOMES-low individuals (top). The frequencies of DH cell populations are shown in the top-right quadrant. (**D**) Longitudinal TIGIT and KLRG1 coexpression in total CD8 T cells from R, NR, and C patients. Means ± SEM are shown. Asterisks denote significant differences between R and NR patients for each visit. Arrows indicate times of initiation of treatment courses. (**E**) Pie charts of the mean fractions of $TIGIT^+KLRG1^+$ cells in each subset at indicated time points.

as compared with only ~85% in DL cells. The cumulative distribution plot for *EOMES*-associated gene expression was shifted significantly to the right in DH cells ($P = 8.4 \times 10^{-11}$, Kolmogorov-Smirnov test), indicating that signature genes were expressed at higher levels in DH than in DL cells.

Characterization of T cell receptor (TCR) CDR3 sequence variation (clonotype) may be used to provide a measure of T cell diversity and antigen specificity (*21*). We used single-cell RNA-seq to determine specificities (TCR sequences or clonotypes) and functional capacities (whole-transcriptome phenotypes) of individual T cells. From the RNA-seq data, we identified TCR clonotypes in DH and DL cells from three R patients. About 86% (219 of 254) good-quality single-cell profiles from individual DH and DL cells yielded rearranged *TRAV* and/or *TRBV* genes, demonstrating that they were αβ T cells (table S4). When sequences of the individual CDR3 junctions were compared (Fig. 3C), DH cells from all three patients showed more extensive clonotype sharing than did DL cells. This finding indicates that DH cells exhibited more in vivo clonal expansion than did DL cells (for clonotypes expressed in more than one cell, $P = 1 \times 10^{-3}$, Fisher's exact test).

It was important to determine whether CD8 T cells expressing *EOMES* network genes were uniquely autoreactive T cells or represented a broader phenomenon observed on CD8 T cells, including those reactive with environmental foreign antigens. To distinguish these possibilities, we performed a BLAST (Basic Local Alignment Search Tool) sequence comparison of CDR3 regions of DH and DL cell TCRs versus the NCBI (National Center for Biotechnology

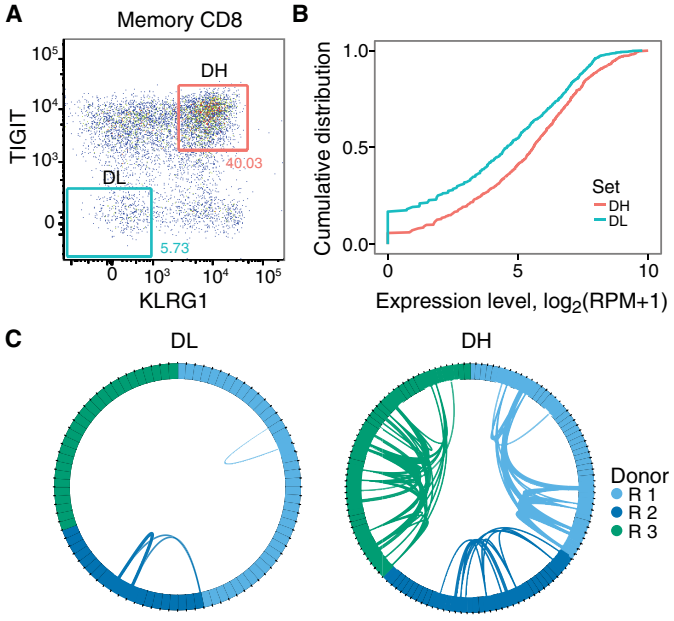

Fig. 3. TIGIT$^+$KLRG1$^+$ CD8 memory T cells from R patients expressed expanded TCRs. (**A**) Gating scheme for isolation of TIGIT$^+$KLRG1$^+$ (DH) and TIGIT$^-$KLRG1$^-$ (DL) populations from CD8 memory (CD8$^+$CD45RO$^+$ of CD3$^+$CD56$^-$) T cells. (**B**) Cumulative distribution plots for the fraction of EOMES network genes detected (*y* axis) versus expression levels (*x* axis). This plot is representative of the three R patients tested; the plot comprises five replicates for DH cells and four replicates for DL cells from a single individual. (**C**) Each segment in the plot represents a library (or cell), yielding a TCR junction from DH cells isolated from three R patients (tables S1 and S4). Arcs connect cells sharing junctions, with line thickness proportional to the number of junctions shared between cells. Responders 1 to 3 yielded 56, 44, and 67 unique junctions, respectively, and 4, 5, and 9 expanded junctions (i.e., expressed more than one cell) for DH cells, and 70, 30, and 49 unique junctions and 1, 2, and 0 expanded junctions for DL cells.

Information) nonredundant protein database. This comparison revealed CDR3 regions that perfectly matched previously described TCR sequences (13 of 315, ~4%), including well-characterized sequences from studies of viruses (*22*, *23*), MAIT cells (which recognize bacterial products) (*24*–*26*), autoantigens (*23*, *27*), and alloantigens (*28*) (table S4). The diversity of these specificities was consistent with the high frequency of TIGIT$^+$KLRG1$^+$ CD8 T cells, which were found at a much higher level than observed for single antigens. Moreover, these data demonstrate that both DH and DL cells represent a broad-based spectrum of CD8 T cell specificities, including both autoimmune and environmental antigens.

CD8 T cells expressing *EOMES*-associated genes phenotypically and functionally resemble partially exhausted cells

To further characterize CD8 T cells expressing *EOMES*-associated genes, we compared the proliferative capacities of DH and DL cells sorted from the same three R patients at month 6. If DH cells functionally resemble effector cells, then we would expect an increase in proliferative capacity. By comparison, if DH cells functionally resemble exhausted cells, then we would expect them to be hypoproliferative. To minimize the amount of rare samples required, we assessed regulation of cell cycle and proliferation genes as a measure of proliferation after stimulation with anti-CD3/anti-CD28 mAbs (polyclonal stimulation), using RNA-seq transcript profiles as the readout. As shown in Fig. 4A, mAb stimulation of DH cells triggered a transcriptional response that included genes implicated in in vivo activation of CD8 T cells (*29*). When compared with DL cells (Fig. 4B), DH cells responded to polyclonal stimulation by up-regulation of IRs and down-regulation of multiple cell cycle genes. Thus, DH cells are less proliferative than DL cells and respond to stimulation by preferential up-regulation of multiple IRs in addition to TIGIT and KLRG1.

Exhausted T cells exhibit characteristic patterns of IR, effector molecule, and transcription factor expression (*6*, *9*, *10*). To examine these features in more detail, we compared expression of selected molecules from low-input bulk profiles (Fig. 4C). In response to stimulation, DH cells expressed significantly higher levels of IR transcripts [*TIGIT*, *KLRG1*, *CD160*, *LAG3*, and *HAVCR2* (TIM3)] than did DL cells; levels of *PDCD1* did not differ between the two cell types. For effector molecules, stimulated DH cells expressed higher levels of *GZMA*, *GZMH*, *GZMK*, and *PRF1* than did DL cells, but *GZMB* and *IFNG* did not differ. For transcription factors, DH cells expressed higher levels of *EOMES*, *MAF*, and *STAT4* but lower levels of *E2F1* and *STAT1* than did DL cells, whereas *TBX21* did not differ between the two cell types.

Although DH cells had less proliferative capacity than DL cells, they nonetheless responded to anti-CD3/anti-CD28 stimulation. This suggested that the elevated IR levels seen from DH cells may make them susceptible to down-modulation upon encountering IR ligands (IRLs). To test this possibility, we treated DH cells with polyclonal stimulation, with or without PVR-Fc, a soluble IRL for TIGIT. PVR-Fc would be expected to bind the IR TIGIT, as well as costimulatory receptors CD226 and CD96, on T cells (*30*). When we added PVR-Fc to anti-CD3/anti-CD28–stimulated cells, we observed regulation of many genes. Genes that were increased by polyclonal stimulation alone were down-regulated by PVR-Fc triggering, as indicated by the negative slope of the comparison for these conditions (Fig. 4D). Thus, PVR-Fc triggering down-regulates genes that are up-regulated by anti-CD3/anti-CD28 triggering in unstimulated cells (Fig. 4A), consistent with delivery of an inhibitory signal with the potential to provide tolerance.

DISCUSSION

Using a combination of systems immunology and flow cytometry approaches, we have shown that successful therapy with teplizumab is associated with a whole-blood gene signature comprising *EOMES*-associated genes. The gene signature is correlated with C-peptide levels, is expressed by a subset of CD8 T cells that accumulate in patients in proportion to their degree of treatment response (R > NR > C), and appears with kinetics mirroring the timing of teplizumab therapy. Therefore, our data indicate that this cell subset is closely associated with successful response to teplizumab therapy.

Combined, the whole-blood gene signature and flow cytometry results indicate an increase in the percentage of CD8 T cells expressing *EOMES* signature genes in peripheral blood of R patients after teplizumab treatment. This observation is supported by the finding that DH cells show significant TCR sharing (Fig. 3C), as would occur during clonal expansion in vivo, consistent with perfect sequence matches to TCRs recognizing known foreign antigens and autoantigens. Support for generation of a novel cell subset as opposed to expansion of a preexisting cell type comes from the finding that *EOMES*-high cells exhibited elevated levels of IRs TIGIT, KLRG1,

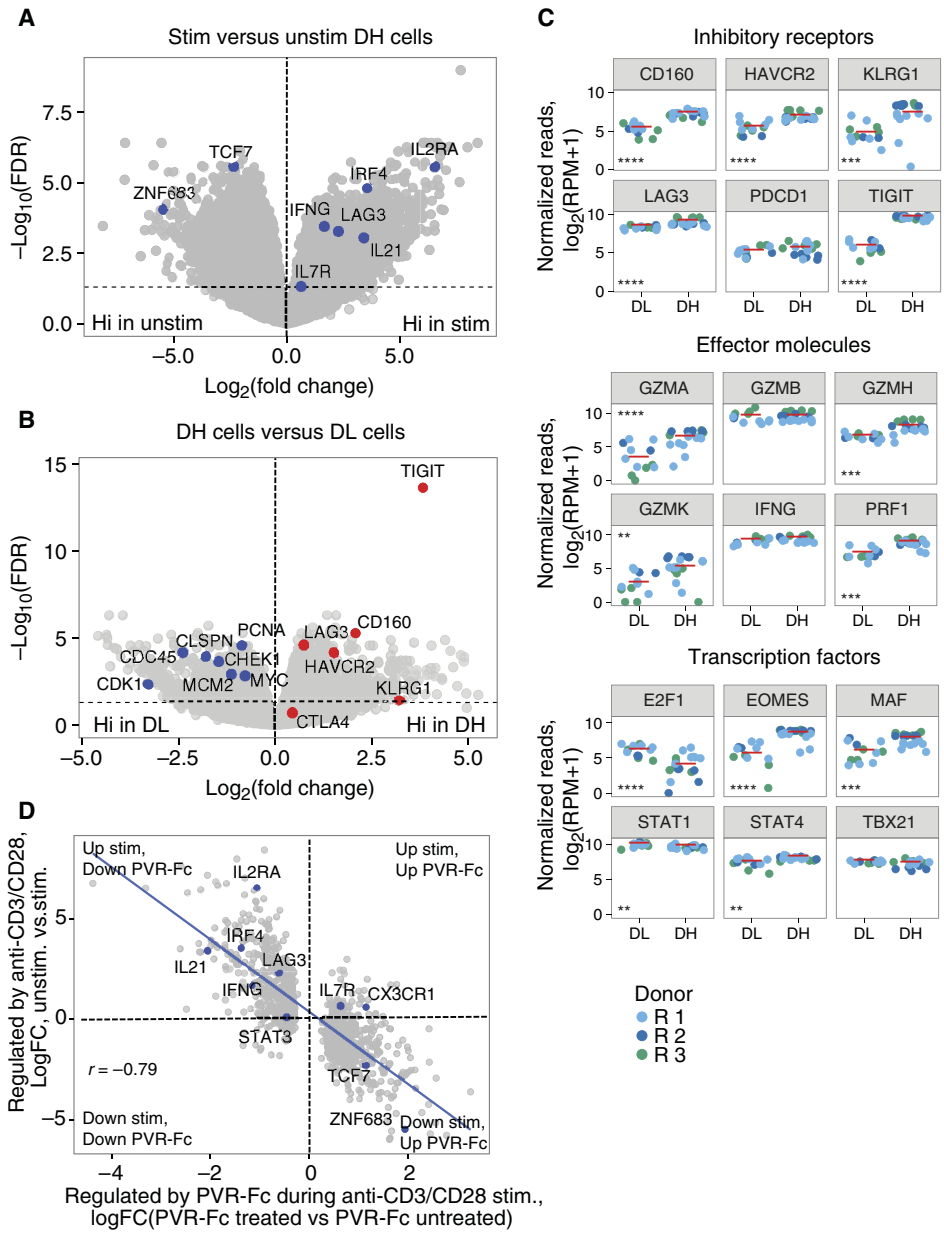

Fig. 4. DH cells up-regulate multiple IRs and down-regulate cell cycle genes during anti-CD3/anti-CD28 stimulation. (**A**) Differential gene expression in anti-CD3/anti-CD28 mAb–stimulated DH cells versus anti-CD3/anti-CD28 mAb–unstimulated DH cells. Blue dots, selected CD8 T cell genes that correlate with T cell expansion in acute EBV infection (*29*); gray dots, all other genes. Horizontal dashed line, FDR = 0.05; vertical dashed line, log(fold change) = 0. (**B**) Differential gene expression in CD3/anti-CD28 mAb–stimulated DH cells versus DL cells. Red dots, selected IR genes; blue dots, selected cell cycle genes; gray dots, all other genes. (**C**) Gene expression of selected IRs (left), effector molecules (middle), and transcription factors (right) in anti-CD3/anti-CD28–stimulated DH and DL cells from three R patients. Horizontal bars, means. Asterisks indicate genes that were detected as differentially expressed by Wilcoxon test (*$P < 0.05$ and *$P \geq 0.01$; **$P < 0.01$ and **$P \geq 0.001$; ***$P < 0.001$ and ***$P \geq 0.0001$; ****$P < 0.0001$). (**D**) *Y* axis, gene regulation [log(fold change)] triggered by stimulation of DH cells (A); *x* axis, gene regulation triggered by anti-CD3/anti-CD28 mAbs ± soluble PVR-Fc. This projection is restricted to genes regulated significantly under both conditions (FDR < 0.05).

and CD160 on naive and memory CD8 T cells (Fig. 2, A and B). Also, we did not detect the *EOMES* signature before therapy (Fig. 1). Likewise, DH cells expressed an increased proportion and higher expression levels of *EOMES*-associated genes than did DL cells (Fig. 3B). The detection of *EOMES* network genes in both populations, albeit at different levels, suggests complexity in the regulation of these genes in different cell populations, perhaps through differential connectivity of *EOMES* in different cell types or activation states (*6*). Together, our data suggest that the CD8 T cells that accumulate in R patients are both qualitatively and quantitatively different from cells that exist in C patients. Elevations of CD8 cell levels with altered functional responses have been noted in other clinical studies with teplizumab (*20*, *31*). It is presently unknown whether increased frequencies of CD8 T cells accompany C-peptide stabilization in clinical studies with other biologic agents.

Previous reports have identified several CD8 T cell populations whose accumulation might delay decline of β cell function in T1D, including CD8 T cells with unique suppressive activity (*32*, *33*), cytotoxic CD8 T cells that could be "CD8 suppressors" by virtue of killing antigen-presenting cells (*34*, *35*), CD8 T cells that regulate response to antigens by other mechanisms (*36*), and a novel CD8 T-NK "hybrid" cell type (*37*). Another possibility is that successful therapies may induce CD8 T cell exhaustion (*9*, *11*) in T1D. In support of this possibility, we found that EBV reactivation correlates with *EOMES* transcript levels, as would be expected if exhausted CD8 T cells could not control chronic viral infection.

The *EOMES*-associated gene-expressing CD8 T cells we identified (DH cells) resemble partially exhausted CD8 T cells in important ways. DH cells sorted from R patients after teplizumab treatment express higher levels of multiple IRs than do DL cells, including *TIGIT*, *KLRG1*, *CD160*, *LAG3*, and *TIM3* (Fig. 4C). Initially, *PDCD1* was proposed as a marker for exhausted T cells (*4*, *38*), but in our studies, *PDCD1* levels do not differ between DH and DL cells (Fig. 4, C and D). An additional feature of DH cells shared with exhausted T cells is that they are hypoproliferative after TCR ligation, compared with DL cells, and respond to polyclonal activation by greater up-regulation of IRs and lower up-regulation of cell cycle genes (Fig. 4B). The fact that DH cells are expanded in R in vivo suggests that treatment with teplizumab induces DH cells, as opposed to expanding a preexisting hypoproliferative population. Although expansion of a hypoproliferative population may seem counterintuitive, the paradox can be explained if the exhaustion phenotype developed subsequent to expansion.

However, DH cells do not exhibit all commonly accepted features of terminally exhausted cells. Exhausted cells are generally

thought to have reduced effector function (*4*, *9*, *11*). Although the effector activity of DH cells is unknown, they express robust levels of effector molecules, especially after polyclonal activation (granzymes, *IFNG*, etc.; Fig. 4C), making it likely that they retain some effector functions. Moreover, DH cells are not fully exhausted, because they are down-modulated by PVR-Fc, a ligand for the IR TIGIT (Fig. 4D). In other systems, there is a requirement for persistent antigen exposure for maintenance of the exhausted phenotype (*4*). However, in R patients, the relationship between CD8 T cells expressing *EOMES*-associated genes and antigen persistence is unclear. Elevated DH cells persisted for many months after treatment, whereas teplizumab is no longer detectable on the surfaces of T cells 2 weeks after completing a 2-week treatment course (*14*).

Together, the coexpression of multiple IRs, reduced but not ablated proliferative capacity, and the ability to be further down-regulated by IR triggering suggest that DH cells have a partially exhausted–like phenotype (*39*). How this is beneficial for T1D patients remains to be elucidated, in particular, how it relates to the status of islet-reactive CD8 T cells in R patients. Our results show correlation, not necessarily causality, between partial CD8 T cell exhaustion and favorable response to therapy in T1D. However, in light of our results, it is reasonable to speculate that the beneficial effects of teplizumab therapy may result in part from partial or transient exhaustion and, consequently, reduced islet autoreactivity of CD8 effector T cells. The absence of a terminally exhausted phenotype suggests a lack of complete cell commitment and is consistent with the transient nature of the clinical effect of teplizumab. In contrast, because partial exhaustion is also seen in foreign antigen–specific cells and correlates with reactivation of EBV, caution should be taken in using anti-CD3 therapy for an extended period of time.

Immunotherapy trials in cancer have shown that agents reversing effector T cell exhaustion to increase antitumor immunity result in marked clinical responses (*40*). One side effect of these anticancer therapies is autoimmune diabetes (*41*), consistent with findings that signatures associated with CD8 T cell exhaustion positively correlate with improved prognosis for autoimmunity (*12*). Therefore, our studies provide primary evidence that pathways clinically important and undesirable for tumor immunology are also potentially important but desirable for response to teplizumab therapy in T1D. Although agents that reverse T cell exhaustion are undergoing intense investigation as antitumor agents (*40*), much less attention has been given to agents that promote and sustain T cell exhaustion as therapies for autoimmune diseases. Our results, together with the proven clinical tractability of this pathway in humans, suggest that enhancing CD8 T cell exhaustion may provide new therapeutic possibilities for T1D and other autoimmune diseases.

MATERIALS AND METHODS

Study design and samples

The AbATE study involved treatment of new-onset T1D patients with teplizumab for 2 weeks at diagnosis and after 1 year in an open-label, randomized, controlled trial. The study design was described previously (*8*), and the complete protocol is available at www.immunetolerance.org. Analysis of EBV reactivation was described previously (*8*).

Samples were collected at timed visits during the study and stored frozen until use. For RNA extraction, whole-blood samples were collected into Tempus tubes (Thermo Fisher Scientific), and RNA was prepared at commercial vendors (Expression Analysis and Fisher). Flow cytometry experiments used frozen PBMCs isolated from whole blood and were viably cryopreserved at the Immune Tolerance Network Core facility. Samples for the present study were distributed by the Immune Tolerance Network and are described in table S1 and at www.itntrialshare.org/. Detailed methods can be found in the Supplementary Materials.

SUPPLEMENTARY MATERIALS

immunology.sciencemag.org/cgi/content/full/1/5/aai7793/DC1

Methods

Fig. S1. Schematic representation of the AbATE trial of teplizumab in newly diagnosed T1D.

Fig. S2. Identifying biological themes enriched in top C-peptide genes.

Fig. S3. An NK/T cell, *EOMES*-associated gene signature was detected in whole blood of teplizumab R patients.

Fig. S4. GSEA shows positive correlation between EOMES.mod and other overlapping modules with the R phenotype.

Fig. S5. Correlation of *EOMES* expression with lymphocyte subset levels.

Fig. S6. Diagram of flow cytometric single-cell analysis of *EOMES*-associated proteins.

Fig. S7. Representative gating for univariate expression analysis by flow cytometry on T and NK cell subsets.

Fig. S8. Representative gating for coexpression longitudinal analysis by flow cytometry.

Table S1. Numbers and characteristics of samples used in this study.

Table S2. *EOMES*-correlated genes.

Table S3. Flow cytometry panels.

Table S4. TCR rearrangements in DH cells versus DL cells.

References (*42*–*55*)

REFERENCES AND NOTES

1. M. R. Rigby, M. R. Ehlers, Targeted immune interventions for type 1 diabetes: Not as easy as it looks! *Curr. Opin. Endocrinol. Diabetes Obes.* **21**, 271–278 (2014).
2. C. J. Greenbaum, D. A. Schatz, M. J. Haller, S. Sanda, Through the fog: Recent clinical trials to preserve β-cell function in type 1 diabetes. *Diabetes* **61**, 1323–1330 (2012).
3. M. Wållberg, A. Cooke, Immune mechanisms in type 1 diabetes. *Trends Immunol.* **34**, 583–591 (2013).
4. J. Crespo, H. Sun, T. H. Welling, Z. Tian, W. Zou, T cell anergy, exhaustion, senescence, and stemness in the tumor microenvironment. *Curr. Opin. Immunol.* **25**, 214–221 (2013).
5. A. Schietinger, P. D. Greenberg, Tolerance and exhaustion: Defining mechanisms of T cell dysfunction. *Trends Immunol.* **35**, 51–60 (2014).
6. T. A. Doering, A. Crawford, J. M. Angelosanto, M. A. Paley, C. G. Ziegler, E. J. Wherry, Network analysis reveals centrally connected genes and pathways involved in $CD8^+$ T cell exhaustion versus memory. *Immunity* **37**, 1130–1144 (2012).
7. Cancer Genome Atlas Network, Comprehensive molecular portraits of human breast tumours. *Nature* **490**, 61–70 (2012).
8. M. E. Ritchie, B. Phipson, D. Wu, Y. Hu, C. W. Law, W. Shi, G. K. Smyth, *limma* powers differential expression analyses for RNA-sequencing and microarray studies. *Nucleic Acids Res.* **43**, e47 (2015).
9. E. J. Wherry, M. Kurachi, Molecular and cellular insights into T cell exhaustion. *Nat. Rev. Immunol.* **15**, 486–499 (2015).
10. A. Crawford, J. M. Angelosanto, C. Kao, T. A. Doering, P. M. Odorizzi, B. E. Barnett, E. J. Wherry, Molecular and transcriptional basis of $CD4^+$ T cell dysfunction during chronic infection. *Immunity* **40**, 289–302 (2014).
11. E. J. Wherry, T cell exhaustion. *Nat. Immunol.* **12**, 492–499 (2011).
12. E. F. McKinney, J. C. Lee, D. R. W. Jayne, P. A. Lyons, K. G. C. Smith, T-cell exhaustion, co-stimulation and clinical outcome in autoimmunity and infection. *Nature* **523**, 612–616 (2015).
13. F. Reynier, A. Pachot, M. Paye, Q. Xu, F. Turrel-Davin, F. Petit, A. Hot, C. Auffray, N. Bendelac, M. Nicolino, B. Mougin, C. Thivolet, Specific gene expression signature associated with development of autoimmune type-I diabetes using whole-blood microarray analysis. *Genes Immun.* **11**, 269–278 (2010).
14. K. C. Herold, S. E. Gitelman, M. R. Ehlers, P. A. Gottlieb, C. J. Greenbaum, W. Hagopian, K. D. Boyle, L. Keyes-Elstein, S. Aggarwal, D. Phippard, P. H. Sayre, J. McNamara, J. A. Bluestone; AbATE Study Team, Teplizumab (anti-CD3 mAb) treatment preserves C-peptide responses in patients with new-onset type 1 diabetes in a randomized controlled trial: Metabolic and immunologic features at baseline identify a subgroup of responders. *Diabetes* **62**, 3766–3774 (2013).

15. P. S. Linsley, C. Speake, E. Whalen, D. Chaussabel, Copy number loss of the interferon gene cluster in melanomas is linked to reduced T cell infiltrate and poor patient prognosis. *PLOS ONE* **9**, e109760 (2014).
16. N. Novershtern, A. Subramanian, L. N. Lawton, R. H. Mak, W. N. Haining, M. E. McConkey, N. Habib, N. Yosef, C. Y. Chang, T. Shay, G. M. Frampton, A. C. B. Drake, I. Leskov, B. Nilsson, F. Preffer, D. Dombkowski, J. W. Evans, T. Liefeld, J. S. Smutko, J. Chen, N. Friedman, R. A. Young, T. R. Golub, A. Regev, B. L. Ebert, Densely interconnected transcriptional circuits control cell states in human hematopoiesis. *Cell* **144**, 296–309 (2011).
17. A. Subramanian, P. Tamayo, V. K. Mootha, S. Mukherjee, B. L. Ebert, M. A. Gillette, A. Paulovich, S. L. Pomeroy, T. R. Golub, E. S. Lander, J. P. Mesirov, Gene set enrichment analysis: A knowledge-based approach for interpreting genome-wide expression profiles. *Proc. Natl. Acad. Sci. U.S.A.* **102**, 15545–15550 (2005).
18. A. Mortazavi, B. A. Williams, K. McCue, L. Schaeffer, B. Wold, Mapping and quantifying mammalian transcriptomes by RNA-Seq. *Nat. Methods* **5**, 621–628 (2008).
19. A. Franceschini, D. Szklarczyk, S. Frankild, M. Kuhn, M. Simonovic, A. Roth, J. Lin, P. Minguez, P. Bork, C. von Mering, L. J. Jensen, STRING v9.1: Protein-protein interaction networks, with increased coverage and integration. *Nucleic Acids Res.* **41**, D808–D815 (2013).
20. J. E. Tooley, N. Vudattu, J. Choi, C. Cotsapas, L. Devine, K. Raddassi, M. R. Ehlers, J. G. McNamara, K. M. Harris, S. Kanaparthi, D. Phippard, K. C. Herold, Changes in T-cell subsets identify responders to FcR-nonbinding anti-CD3 mAb (teplizumab) in patients with type 1 diabetes. *Eur. J. Immunol.* **46**, 230–241 (2016).
21. S. J. Turner, P. C. Doherty, J. McCluskey, J. Rossjohn, Structural determinants of T-cell receptor bias in immunity. *Nat. Rev. Immunol.* **6**, 883–894 (2006).
22. G. B. Stewart-Jones, P. Simpson, P. A. van der Merwe, P. Easterbrook, A. J. McMichael, S. L. Rowland-Jones, E. Y. Jones, G. M. Gillespie, Structural features underlying T-cell receptor sensitivity to concealed MHC class I micropolymorphisms. *Proc. Natl. Acad. Sci. U.S.A.* **109**, E3483–E3492 (2012).
23. T. Schneider-Hohendorf, H. Mohan, C. G. Bien, J. Breuer, A. Becker, D. Görlich, T. Kuhlmann, G. Widman, S. Herich, C. Elpers, N. Melzer, K. Dornmair, G. Kurlemann, H. Wiendl, N. Schwab, CD8$^+$ T-cell pathogenicity in Rasmussen encephalitis elucidated by large-scale T-cell receptor sequencing. *Nat. Commun.* **7**, 11153 (2016).
24. S. B. G. Eckle, R. W. Birkinshaw, L. Kostenko, A. J. Corbett, H. E. G. McWilliam, R. Reantragoon, Z. Chen, N. A. Gherardin, T. Beddoe, L. Liu, O. Patel, B. Meehan, D. P. Fairlie, J. A. Villadangos, D. I. Godfrey, L. Kjer-Nielsen, J. McCluskey, J. Rossjohn, A molecular basis underpinning the T cell receptor heterogeneity of mucosal-associated invariant T cells. *J. Exp. Med.* **211**, 1585–1600 (2014).
25. S. Porcelli, C. E. Yockey, M. B. Brenner, S. P. Balk, Analysis of T cell antigen receptor (TCR) expression by human peripheral blood CD4-8- α/β T cells demonstrates preferential use of several Vβ genes and an invariant TCR α chain. *J. Exp. Med.* **178**, 1–16 (1993).
26. N. A. Gherardin, A. N. Keller, R. E. Woolley, J. Le Nours, D. S. Ritchie, P. J. Neeson, R. W. Birkinshaw, S. B. G. Eckle, J. N. Waddington, L. Liu, D. P. Fairlie, A. P. Uldrich, D. G. Pellicci, J. McCluskey, D. I. Godfrey, J. Rossjohn, Diversity of T cells restricted by the MHC class I-related molecule MR1 facilitates differential antigen recognition. *Immunity* **44**, 32–45 (2016).
27. M. L. Joachims, K. M. Leehan, C. Lawrence, R. C. Pelikan, J. S. Moore, Z. Pan, A. Rasmussen, L. Radfar, D. M. Lewis, K. M. Grundahl, J. A. Kelly, G. B. Wiley, M. Shugay, D. M. Chudakov, C. J. Lessard, D. U. Stone, R. H. Scofield, C. G. Montgomery, K. L. Sivils, L. F. Thompson, A. D. Farris, Single-cell analysis of glandular T cell receptors in Sjögren's syndrome. *JCI Insight* **1**, e85609 (2016).
28. J.-W. Du, J.-Y. Gu, J. Liu, X.-N. Cen, Y. Zhang, Y. Ou, B. Chu, P. Zhu, TCR spectratyping revealed T lymphocytes associated with graft-versus-host disease after allogeneic hematopoietic stem cell transplantation. *Leuk. Lymphoma* **48**, 1618–1627 (2007).
29. T. C. Greenough, J. R. Straubhaar, L. Kamga, E. R. Weiss, R. M. Brody, M. M. McManus, L. K. Lambrecht, M. Somasundaran, K. F. Luzuriaga, A gene expression signature that correlates with CD8$^+$ T cell expansion in acute EBV infection. *J. Immunol.* **195**, 4185–4197 (2015).
30. S. A. Fuertes Marraco, N. J. Neubert, G. Verdeil, D. E. Speiser, Inhibitory receptors beyond T cell exhaustion. *Front. Immunol.* **6**, 310 (2015).
31. V. Ablamunits, K. C. Herold, Generation and function of human regulatory CD8+ T cells induced by a humanized OKT3 monoclonal antibody hOKT3γ1 (Ala-Ala). *Hum. Immunol.* **69**, 732–736 (2008).
32. H.-J. Kim, X. Wang, S. Radfar, T. J. Sproule, D. C. Roopenian, H. Cantor, CD8$^+$ T regulatory cells express the Ly49 Class I MHC receptor and are defective in autoimmune prone B6-Yaa mice. *Proc. Natl. Acad. Sci. U.S.A.* **108**, 2010–2015 (2011).
33. H. Jiang, S. M. Canfield, M. P. Gallagher, H. H. Jiang, Y. Jiang, Z. Zheng, L. Chess, HLA-E–restricted regulatory CD8$^+$ T cells are involved in development and control of human autoimmune type 1 diabetes. *J. Clin. Invest.* **120**, 3641–3650 (2010).
34. G. Guarda, M. Hons, S. F. Soriano, A. Y. Huang, R. Polley, A. Martín-Fontecha, J. V. Stein, R. N. Germain, A. Lanzavecchia, F. Sallusto, L-selectin-negative CCR7$^-$ effector and memory CD8$^+$ T cells enter reactive lymph nodes and kill dendritic cells. *Nat. Immunol.* **8**, 743–752 (2007).
35. S. Laffont, J. D. Coudert, L. Garidou, L. Delpy, A. Wiedemann, C. Demur, C. Coureau, J.-C. Guéry, CD8$^+$ T-cell–mediated killing of donor dendritic cells prevents alloreactive T helper type-2 responses in vivo. *Blood* **108**, 2257–2264 (2006).
36. B. Bisikirska, J. Colgan, J. Luban, J. A. Bluestone, K. C. Herold, TCR stimulation with modified anti-CD3 mAb expands CD8$^+$ T cell population and induces CD8$^+$CD25$^+$ Tregs. *J. Clin. Invest.* **115**, 2904–2913 (2005).
37. H. Yuling, X. Ruijing, J. Xiang, L. Li, C. Lang, X. Jie, X. Wei, W. Yujuan, Z. Lijun, Z. Rui, T. Xinti, B. Yongyi, J. Yan-Ping, J. Youxin, T. Jinquan, EBV promotes human CD8$^+$ NKT cell development. *PLOS Pathog.* **6**, e1000915 (2010).
38. D. L. Barber, E. J. Wherry, D. Masopust, B. Zhu, J. P. Allison, A. H. Sharpe, G. J. Freeman, R. Ahmed, Restoring function in exhausted CD8 T cells during chronic viral infection. *Nature* **439**, 682–687 (2006).
39. E. J. Wherry, S.-J. Ha, S. M. Kaech, W. N. Haining, S. Sarkar, V. Kalia, S. Subramaniam, J. N. Blattman, D. L. Barber, R. Ahmed, Molecular signature of CD8$^+$ T cell exhaustion during chronic viral infection. *Immunity* **27**, 670–684 (2007).
40. D. S. Chen, I. Mellman, Oncology meets immunology: The cancer-immunity cycle. *Immunity* **39**, 1–10 (2013).
41. J. Hughes, N. Vudattu, M. Sznol, S. Gettinger, H. Kluger, B. Lupsa, K. C. Herold, Precipitation of autoimmune diabetes with anti-PD-1 immunotherapy. *Diabetes Care* **38**, e55–e57 (2015).
42. P. Du, W. A. Kibbe, S. M. Lin, *lumi*: A pipeline for processing Illumina microarray. *Bioinformatics* **24**, 1547–1548 (2008).
43. P. Du, W. A. Kibbe, S. M. Lin, nuID: A universal naming scheme of oligonucleotides for illumina, Affymetrix, and other microarrays. *Biol. Direct* **2**, 16 (2007).
44. P. Langfelder, S. Horvath, WGCNA: An R package for weighted correlation network analysis. *BMC Bioinf.* **9**, 559 (2008).
45. A. R. Wu, N. F. Neff, T. Kalisky, P. Dalerba, B. Treutlein, M. E. Rothenberg, F. M. Mburu, G. L. Mantalas, S. Sim, M. F. Clarke, S. R. Quake, Quantitative assessment of single-cell RNA-sequencing methods. *Nat. Methods* **11**, 41–46 (2014).
46. B. Giardine, C. Riemer, R. C. Hardison, R. Burhans, L. Elnitski, P. Shah, Y. Zhang, D. Blankenberg, I. Albert, J. Taylor, W. Miller, W. J. Kent, A. Nekrutenko, Galaxy: A platform for interactive large-scale genome analysis. *Genome Res.* **15**, 1451–1455 (2005).
47. E. Afgan, D. Baker, M. van den Beek, D. Blankenberg, D. Bouvier, M. Čech, J. Chilton, D. Clements, N. Coraor, C. Eberhard, B. Grüning, A. Guerler, J. Hillman-Jackson, G. Von Kuster, E. Rasche, N. Soranzo, N. Turaga, J. Taylor, A. Nekrutenko, J. Goecks, The Galaxy platform for accessible, reproducible and collaborative biomedical analyses: 2016 update. *Nucleic Acids Res.* **44**, W3–W10 (2016).
48. C. Trapnell, L. Pachter, S. L. Salzberg, TopHat: Discovering splice junctions with RNA-Seq. *Bioinformatics* **25**, 1105–1111 (2009).
49. S. Anders, P. T. Pyl, W. Huber, HTSeq—A Python framework to work with high-throughput sequencing data. *Bioinformatics* **31**, 166–169 (2015).
50. M. D. Robinson, A. Oshlack, A scaling normalization method for differential expression analysis of RNA-seq data. *Genome Biol.* **11**, R25 (2010).
51. M. D. Robinson, D. J. McCarthy, G. K. Smyth, edgeR: A Bioconductor package for differential expression analysis of digital gene expression data. *Bioinformatics* **26**, 139–140 (2010).
52. C. W. Law, Y. Chen, W. Shi, G. K. Smyth, voom: Precision weights unlock linear model analysis tools for RNA-seq read counts. *Genome Biol.* **15**, R29 (2014).
53. M. G. Grabherr, B. J. Haas, M. Yassour, J. Z. Levin, D. A. Thompson, I. Amit, X. Adiconis, L. Fan, R. Raychowdhury, Q. Zeng, Z. Chen, E. Mauceli, N. Hacohen, A. Gnirke, N. Rhind, F. di Palma, B. W. Birren, C. Nusbaum, K. Lindblad-Toh, N. Friedman, A. Regev, Full-length transcriptome assembly from RNA-Seq data without a reference genome. *Nat. Biotechnol.* **29**, 644–652 (2011).
54. X. Brochet, M.-P. Lefranc, V. Giudicelli, IMGT/V-QUEST: The highly customized and integrated system for IG and TR standardized V-J and V-D-J sequence analysis. *Nucleic Acids Res.* **36**, W503–W508 (2008).
55. P. Shannon, A. Markiel, O. Ozier, N. S. Baliga, J. T. Wang, D. Ramage, N. Amin, B. Schwikowski, T. Ideker, Cytoscape: A software environment for integrated models of biomolecular interaction networks. *Genome Res.* **13**, 2498–2504 (2003).

Acknowledgments: We acknowledge D. Phippard and T. Debnam for assistance in obtaining samples, members of the Benaroya Research Institute Genomics and Human Immunophenotyping core facilities for performing laboratory experiments, J. Pardo and N. Lim for assistance with flow cytometry analysis, M. Dufort and S. Murray for comments on the manuscript, and A. Hocking for assistance in preparing the manuscript. **Funding:** This work was funded by NIH grants 1DP3DK104465 and 5UM1AI109565, awarded to P.S.L. and G.T.N., respectively. The work described in this manuscript was partially funded by and will support the mission of the Immune Tolerance Network, which is to accelerate the clinical development of immune tolerance therapies. Salary support for K.C.H. was provided by grant R01DK057846. **Author contributions:** J.T. performed laboratory experiments; V.G. directed the microarray and RNA-seq profiling; J.A.E. performed pipeline analysis of the

RNA-seq data; P.S.L. and H.A.D. analyzed the molecular profiling data; S.A.L., J.T., and H.A.D. analyzed the flow cytometry experiments; K.C.H., M.E., and G.T.N. aided in data interpretation; and P.S.L. and S.A.L. conceived the experiments and wrote the manuscript. All authors made contributions to the final manuscript. **Competing interests:** The authors declare that they have no competing interests. **Data and materials availability:** Data from retained profiles have been deposited in the Gene Expression Omnibus repository (GSE85530 and GSE85531). Data files and R code used to generate figures were deposited in a GitHub repository (https://github.com/linsleyp/Long_Linsley_AbATE).

Submitted 10 August 2016
Accepted 15 October 2016
Published 18 November 2016
10.1126/sciimmunol.aai7793

Citation: S. A. Long, J. Thorpe, H. A. DeBerg, V. Gersuk, J. A. Eddy, K. M. Harris, M. Ehlers, K. C. Herold, G. T. Nepom, P. S. Linsley, Partial exhaustion of CD8 T cells and clinical response to teplizumab in new-onset type 1 diabetes. *Sci. Immunol.* **1**, eaai7793 (2016).

Science Immunology
AAAS

Partial exhaustion of CD8 T cells and clinical response to teplizumab in new-onset type 1 diabetes

S. Alice Long, Jerill Thorpe, Hannah A. DeBerg, Vivian Gersuk, James A. Eddy, Kristina M. Harris, Mario Ehlers, Kevan C. Herold, Gerald T. Nepom and Peter S. Linsley

*Sci. Immunol.*1, (2016)
doi: 10.1126/sciimmunol.aai7793

Editor's Summary Exhausting autoimmunityCheckpoint inhibitors have revolutionized cancer immunotherapy, allowing potentially exhausted tumor-reactive T cells to attack the tumor. However, in the case of autoimmunity, exhausted T cells may be the answer to stopping the disease. Long et al. report that, in type 1 diabetics treated with the anti-CD3 monoclonal antibody teplizumab, CD8 T cells with features of exhausted T cells are associated with best response to treatment. These cells recognized a broad spectrum of autoantigens and proliferated at a lower level ex vivo, yet their exhausted phenotype was not terminal because stimulating these cells with a ligand for the inhibitory receptor TIGIT further down-regulated their activation. These data suggest inducing T cell exhaustion as a potential therapeutic approach for type 1 diabetes.

Science Immunology (ISSN 2375-2548) publishes new articles weekly. The journal is published by the American Association for the Advancement of Science (AAAS), 1200 New York Avenue NW, Washington, DC 20005.